

Jurnal Sainstech Nusantara

https://nusantarajournal.id/sainstech

Vol. 2 No. 3 (2025) 17-34

ISSN: 3063-0657

Aerodynamic Performance Optimization on NACA 2412 Airfoil Flap With The Addition of Riblets

Almer Faadihillah^{1*}, Setyo Hariyadi Suranto Putro¹, Ajeng Wulansari

¹Aircraft Engineering Department, Aviation Polytechnic Surabaya, Jemur Andayani I Street, Surabaya, 60236, INDONESIA

Article Info

Article history:

Received 01 January, 2025 Revised 10 February, 2025 Accepted 20 June, 2025

Abstract

The development of technology in the world of aerodynamics, one of which is research on airfoils. There have been many various studies that have been used to examine airfoils in various flap configurations according to their use. along with the development of the times, research is increasingly easy to do without taking up a lot of time and spending a lot of money. Aerodynamic characteristics are very important in the field of aerodynamic application science aimed at obtaining the maximum performance of an airfoil shape. Therefore, in this case, research on the aerodynamic characteristics of an airfoil is very necessary to get results in the form of airfoil configuration development with force output results for better performance. The results of this study indicate that there is an increase in the performance of NACA 2412 airfoil with the addition of v-groove riblets compared to without v-groove riblets. The existence of v-groove riblets, can delay the occurrence of separation. The simulation shows that the highest lift coefficient increase occurs at $\alpha = 14^{\circ}$ with an increase of 3% lift coefficient and can reduce drag by 7.3% at $\alpha = 2^{\circ}$ so it can be concluded by adding riblets to the airfoil can improve the performance of the Airfoil.

Keyword: Arifoil, NACA 2412, Riblets, Aerodynamic Performance

*Corresponding Author:

Name Almer Faadihillah

Email: Faadihilahalmer069@poltekbangsby.ac.id

1. Introduction

In bionic flow resistance reduction technology, a regular microstructure corresponding to a biological surface is designed to reduce flow resistance by controlling the turbulent structure of the boundary layer [2] and reducing turbulent kinetic energy (TKE). This method has the advantages of simplicity, low energy consumption, and low cost; so it is widely used in aerospace, transportation, transportation, manufacturing industry, and other fields [1]. Passive drag reduction using streamwise riblet surfaces is partly inspired by the natural ribbed surfaces observed in sharks [3], whose textured rib surfaces achieve drag reduction by affecting the flow field pattern and the loss of turbulent kinetic energy in the turbulent boundary layer. The analysis of the turbulence mechanism near the structure wall for drag reduction on riblet surfaces has theoretical guidance for improving energy efficiency.

17

DOI: https://doi.org/10.71225/jstn.v2i3.118

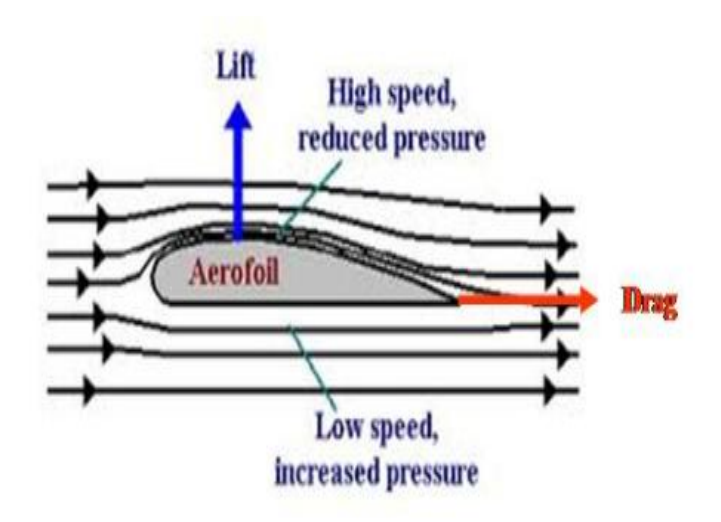


Figure 1. Airfoil Cross Section

In this research, a study was conducted on the airflow on the aircraft wing after the addition of riblets using ANSYS software. Riblets are roughness contours on the surface of the flow path, namely 3 wings. Riblets are regular grooves that have thickness and width. The use of riblets can minimize drag, it depends on the configuration of the thickness and width of a riblets. So the use of riblets is still rarely used [4]. Developments in research use computation to facilitate the calculation of an airfoil. One of the methods used in computing is the Computational Fluid Dynamic (CFD) method. There are many types of specialized software for calculating fluid problems with the CFD method. The result is an approximation of the value of each variable at a certain point in the domain. To solve equations in CFD (Computional Fluid Dynamic) analysis, software can be used for problems in fluid dynamics, including Solidwork, Exceed, GAMBIT, CATIA, NASTRAN, ProEngineering, ANSYS, and others. There are many types of specialized software for calculating fluid problems with CFD methods. The result is an approximation of the value of each variable at a specific point in the domain. To solve equations in CFD (Computional Fluid Dynamic) analysis, software can be used for problems in fluid dynamics, including Solidwork, Exceed, GAMBIT, CATIA, NASTRAN, ProEngineering, ANSYS, and others.

In this research, a study was conducted on the airflow on the aircraft wing after the addition of v-groove riblets on the flap with NACA 2412 airfoil using ANSYS software. Riblets are roughness contours on the surface of the flow path, namely the wing. Riblets are regular grooves that have thickness and width. The use of riblets can increase and decrease the drag force, it depends on the configuration of the thickness and width of a riblets. So the use of riblets is still rarely used. The simulation results will be in the form of lift value, drag value, and visualization of velocity distribution contours. ANSYS is software with a package program that can model finite elements to solve problems related to aerodynamics, including fluid problems. Analysis of the aerodynamic performance of an airfoil cross section is needed to determine the maximum lift that occurs and the forces acting on the airfoil cross section such as lift and drag.

The NACA 2412 airfoil is used on the wing of the Cessna 172 aircraft. The Cessna 172 is a two-seat high wing tricycle general aviation aircraft, designed for flight training, touring and personal use. The Cessna 172 uses piston engines. The aircraft has a capacity of 2 passengers in a single class configuration. One effective way to reduce turbulence and friction on the skin is to modify the addition of extensions in the form of riblets on the wing. delayed separation will increase the lift force

and decrease the drag force on the airfoil so as to improve the performance of the airfoil. With good airfoil performance, it will save fuel for the aircraft when operating.

In this research, a solution was chosen, studying the problem of aerodynamic characteristics around airfoils using ANSYS software with NACA 2412 airfoil test objects by adding V-groove riblets with a chord line of 100 mm and a wing span of 500 mm. One of the reasons for using this software is because, both modeling, meshing process, setting boundary conditions, solving and plotting can be done in an integrated manner with just one software. An airfoil cross section design using ANSYS software with input velocity, angle of attack, viscosity and fluid density so that the difference and efficiency between each test object can be known. The velocity contours obtained in ANSYS are then presented in visual form and compared to determine the differences in characteristics that occur between the 2 (two) test objects..

This research is expected to be useful in the world of aviation, especially those related to aerodynamics on aircraft wings so that this modeling can maximize the flight performance of an aircraft and allow the development of aircraft wing designs that are in accordance with the total design selection with NACA standards. Based on the above background, then in this final project decided to analyze the effect of the use and variation of riblet shapes on aircraft wings with airflow simulations using ANSYS software. The performance of a riblets will produce bound vortex or also called lifting vortex. Bound vortex occurs due to sudden changes in velocity on the airfoil and due to pressure differences. As a result of this bound vortex, the flow above the surface will get additional speed, and the flow below the surface will get a speed reduction. Because of the speed difference, in accordance with Bernoulli's law, there is a force that is directed upwards and is called an elevator.

2. Materials and Method

2.1 Place and Time of Research

This research was located and conducted at the Aviation Polytechnic of Surabaya which is located at JI Jemur Andayani I No 73 Siwalankerto Wonocolo Surabaya, East Java. The location was chosen because of the efficiency of the time for conducting this research which coincided with the author's learning activities.

The research was carried out for 2 (two) semesters at the author's final level, starting from the odd semester of the 2022 / 2023 academic year, namely December 2023 to the end of the even semester of the 2023 / 2024 academic year, namely October 2024

2.2 Data Collection Techniques

The data needed to work on the Final Project is collected from various sources, including through previous research references and searching for data from the internet.

Data collection in this final project research is computationally using the CFD (Computational Fluid Dynamics) method, in the form of airflow simulations on test objects in the form of airfoils. The data taken are the value of the lift force, the value of the drag force, and the contour of the velocity distribution on the test object after the simulation running process. The following is a description of the stages of data collection techniques:

2.3 Research instruments

2.3.1 Hardware

In the process, this research is supported by a device in the form of an Acer Nito V15 Laptop with the following specifications

Table 1. Specifications of research support devices

No	Name	Specification
1	CPU	Intel Core i5-13420H, 8 core (4p + 4e) 12 thread,
		4,6 GHz boost
2	OS	Windows 11 Home
3	Memory	DDR 5, 8 GB
4	Storage	SSD NVMe, 512 GB
5	Graphics	Nvidia GeForce RTX 2050, 4 GB GDDR6

Table 2. Minimum requirement software ansys

No	Name	Specification			
1.	CPU	64-bit Intel or AMD system			
2.	OS	Windows 10			
3.	Memory	8GB RAM			
4.	Storage	512GB			
5.	Graphics	NVIDIA Quadro or AMD Radeon Pro			

2.3.1 Software

The research employed a combination of software tools to support design and simulation processes. Coordinate geometry was initially plotted using *Notepad* to establish the fundamental geometric framework. Data organization and tabulation were conducted in *Microsoft Excel 2021*, which also facilitated preliminary numerical processing. The three-dimensional geometry of the model was then developed using *SolidWorks 2023* to ensure accurate representation of the design specifications. Finally, numerical simulations were performed in *ANSYS R23* to evaluate the structural performance, loading response, and overall validation of the developed design. This integrated software workflow enabled a systematic and reliable computational approach throughout the study.

2.4 Data Analysis Technique

After the data analysis process and discussion based on the simulation data, the simulation data obtained will be in the form of velocity contours, lift values and drag values. From this data, it is processed to see how the effect of adding riblets extensions and variations in the shape applied to the pressure and velocity distribution that can be seen from the contours. And for more advanced how the overall effect on the effectiveness of airfoil work in the form of a comparison table of 2 variations of test objects applied in research simulations. Every data that has been obtained from the results of numerical simulations using the CFD program must be validated. There are three main parameters in the data validation stage, namely: Convergence is defined as determining the number of iterations before CFD calculations are performed. This step is carried out at the flow solver stage, which is the stage of determining the various boundary conditions that must be applied before the simulation process is carried out. The number of iterations used affects the amount of time required for the simulation process. The more number of iterations applied, the more time is needed for the simulation process. The number of iterations required is directly proportional to the total number of

elements used in the modeling process. The more the total number of elements/grids used, the more iterations are needed..

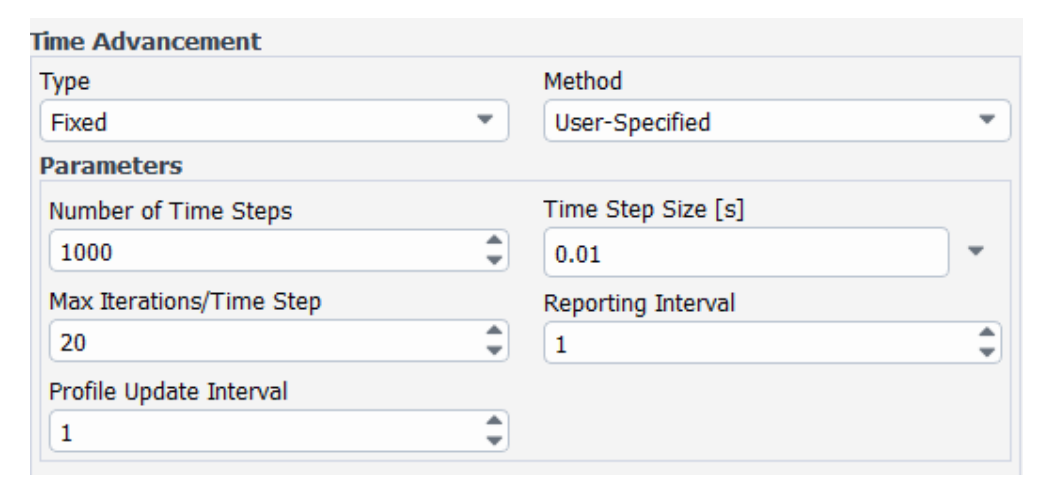


Figure 2. Number of Iterations

At this stage, iteration is carried out until the convergence criterion is 10-6. To get the results correctly, 20-25 time steps are required for each cycle. In this iterate calculation, the Strouhal number is required. Strouhal number is one of the important components in the case of unsteady flow analysis. Strouhal number is obtained from the calculation of the lift coefficient. Strouhal number calculation is as follows:

Periode

$$f = \frac{T_{n-}T_1}{shedding\ cycle} \tag{1}$$

$$f = \frac{1}{Periode} \tag{2}$$

$$St = \frac{f c}{U} \tag{3}$$

Description:

Tn = Time to complete data collection on the lift coefficient graph (seconds)

T1 = Start time of data collection on the lift coefficient graph (seconds)

Shedding cycle = Discharge cycles based on the number of valleys and mountains (cycles) on the CL chart at the particular time taken.

f = Frequency (Hz)

St = Strouhal number

U = Freestream velocity (m/s)

Based on the research of Yarusevych and Boutilier (2011), Strouhal number for airfoils at an angle of 0° is: 0,18

$$S_t = 0.18 = \frac{f c}{U} = 0.036 = 0.36 \text{ m}$$
 (4)
 $U = 72 \text{ m/s}$

F = 50

Cycle Time

$$T = \frac{1}{f} = \frac{1}{50} = 0.02 \text{ sec}$$
 (5)

Time Step Size

$$\frac{0.02}{25} = 8 \times 10^{-4} \text{ sec}$$
 (6)

In the numerical simulation, the maximum number of iterations per step was set to 20, with a total of 1000 time steps. The iteration process may terminate either when the maximum number of iterations is reached or when the specified convergence criterion is satisfied. Optimal convergence is achieved when the process terminates due to meeting the convergence requirement rather than reaching the iteration limit. To ensure accuracy and efficiency of the numerical model, a grid independence study was conducted to determine the most appropriate mesh density and structure. This procedure aims to achieve a mesh resolution at which further refinement produces negligible variations in the solution, thereby confirming that the results are independent of the grid size. In this study, several mesh configurations were tested, and the grid independence was evaluated by comparing the numerical drag coefficient ($\mathcal{C}d$) obtained from each mesh type, with the optimal grid determined from the smallest deviation among the tested cases.

% **Y**+ Meshig Number of Coefficient Inflation Skewness name Cells Drag Layer Average Meshing A 618395 0.0264493 40 0.104763 0,27464 0,433% Meshing B 716010 0.0264581 40 0.104813 0,25457 Meshing C 0.0263920 0,009% 40 0.10488 0,24246 818733 Meshing D 0,003% 40 0,23437 918560 0.0260907 0.104870 Meshing E 0.0262192 0,003% 40 0.105466 0,22892 1026271

Table 3. Grid Independence Test Results

Table 4 shows the results of Grid Independecy on airfoil riblets. Based on table 4, the Cd value that tends to be constant occurs in Meshing D. One consideration in performing numerical simulations is the time and memory used, as well as the smallest Cd, the meshing used for further simulations is Meshing D.

Verification with experimental data was carried out to ensure that the numerical simulation results are reliable and consistent with physical behavior. The accuracy of the model depends strongly on achieving grid independence with an optimal and efficient mesh structure, so that the computational results closely approximate the experimental outcomes. However, it is recognized that discrepancies between simulation and experimental results may still occur. To minimize such deviations, improvements were made by refining the mesh size and adjusting the geometry to better represent the actual configuration. Common sources of error identified in the verification process include the meshing procedure, inaccuracies in data input, and improper definition of boundary conditions. Since these factors significantly influence the final outcome of the simulation, any error in one of them inevitably leads to considerable differences from the experimental results.

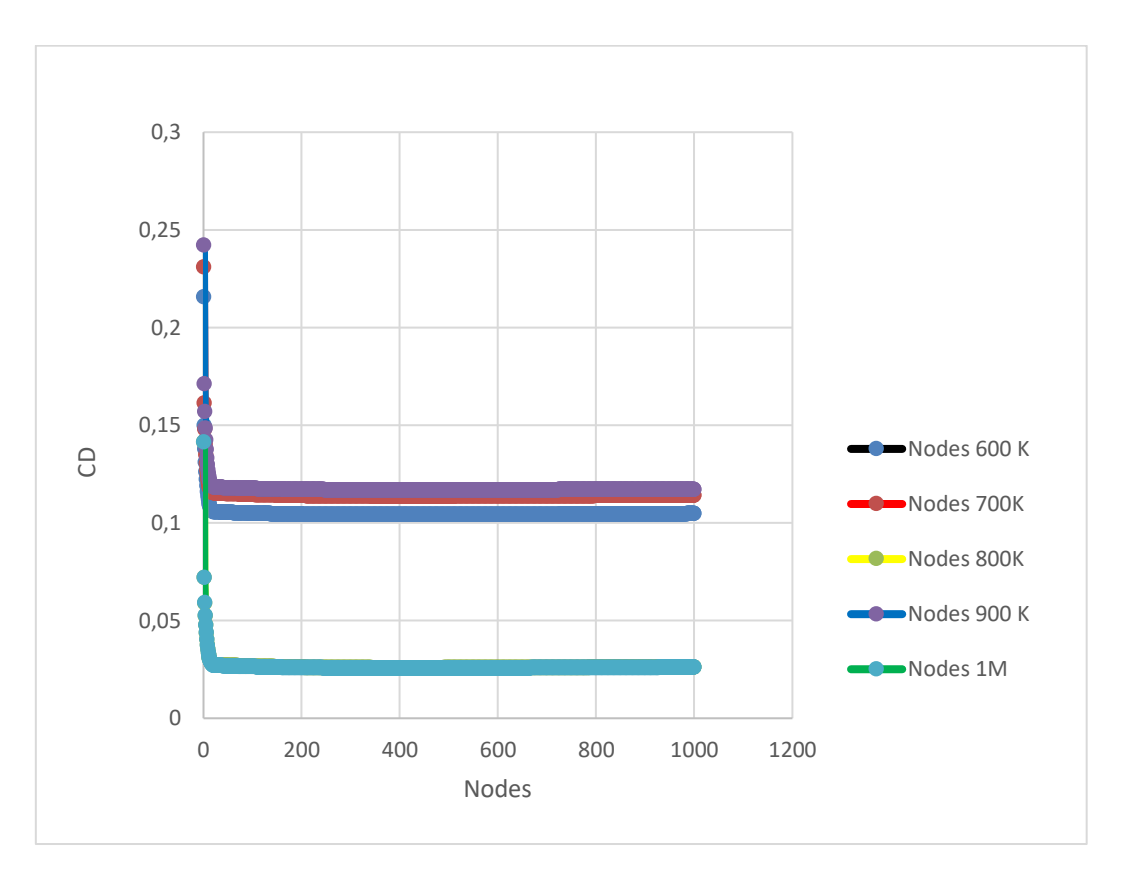


Figure 3. Nodes Comparison

2.5 Pre-Processing Phase

The pre-processing stage represents the initial and fundamental step in constructing and analyzing a Computational Fluid Dynamics (CFD) model. In this study, the pre-processing phase involved the development of two geometric test objects: (1) a NACA 2412 airfoil plain flap equipped with v-groove riblets, and (2) a NACA 2412 airfoil plain flap without v-groove riblets. The preparation of these geometries was followed by detailed pre-processing procedures, which included defining the computational domain, generating the mesh, specifying boundary conditions, and preparing the model for subsequent numerical simulation.

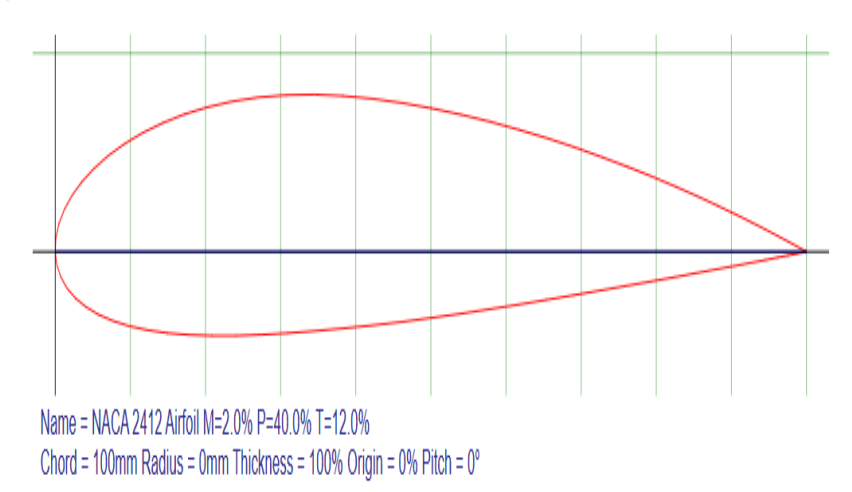


Figure 4. Data Airfoil NACA 2412

At this stage, the process began with collecting and preparing the data required to generate the airfoil geometry. The data were first processed using Microsoft Excel to create a file compatible with SolidWorks, which was then used to construct the NACA 2412 airfoil profile. The curve file was imported into SolidWorks to form the two-dimensional geometry of the airfoil, after which the span and flap were assembled using the mating function. The two-dimensional test piece was subsequently extruded to generate a three-dimensional model. Riblets were created on the flap by sketching and extruding them to the desired dimensions, followed by applying a patterning process to replicate the riblets uniformly along the surface. The riblets and flap were then combined into a single integrated unit. As a result, two geometric test models were developed: (1) the NACA 2412 airfoil plain flap with v-groove riblets, and (2) the NACA 2412 airfoil plain flap without v-groove riblets. The detailed geometric characteristics of each model are described below.

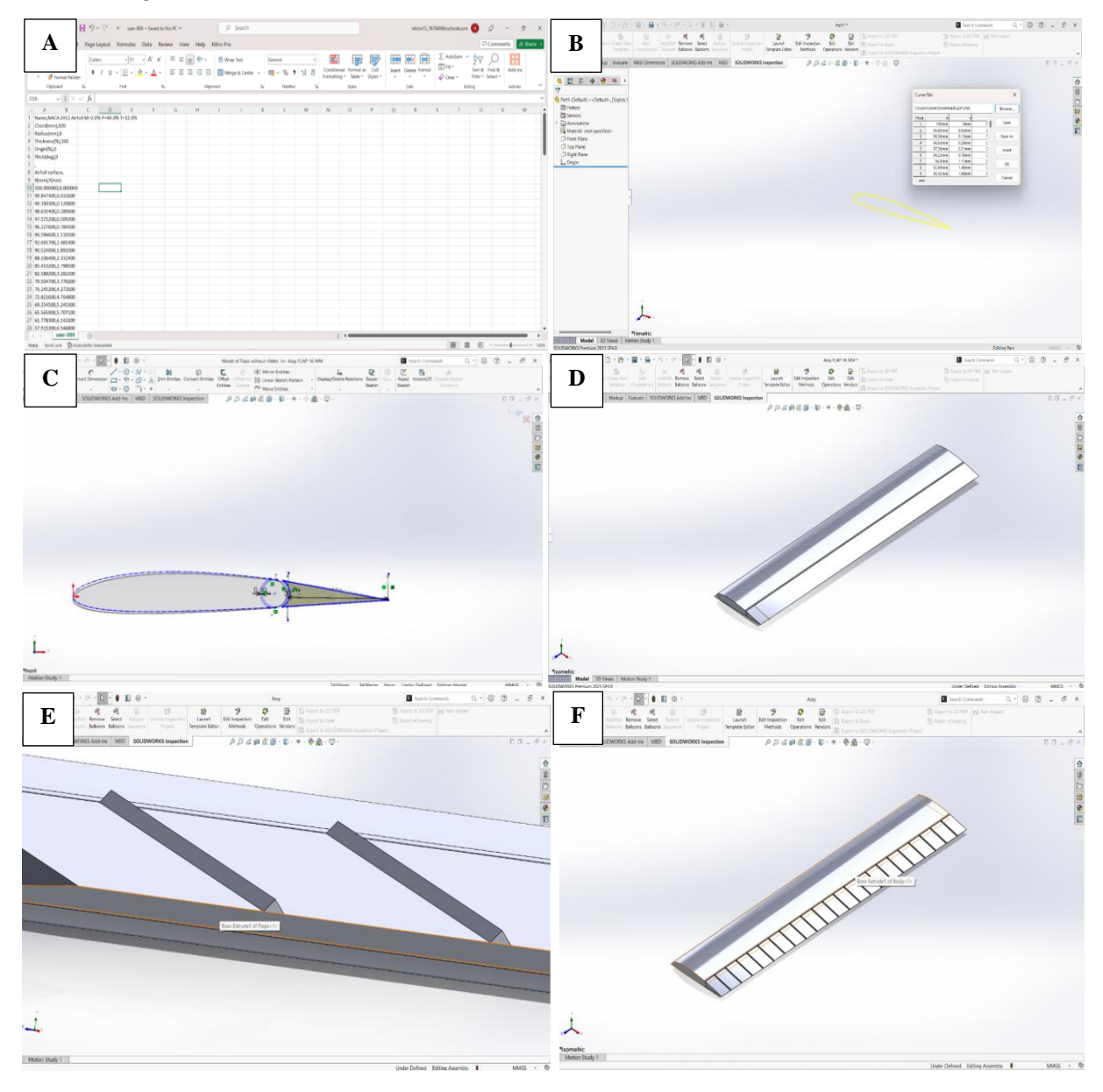


Figure 5. Geometric modeling process of the NACA 2412 airfoil: (a) airfoil coordinate data in Microsoft Excel, (b) imported airfoil geometry in SolidWorks, (c) assembly of flap and span, (d) extrusion of the NACA 2412 airfoil, and (e) riblet formation on the flap surface (f) Duplicate Riblets

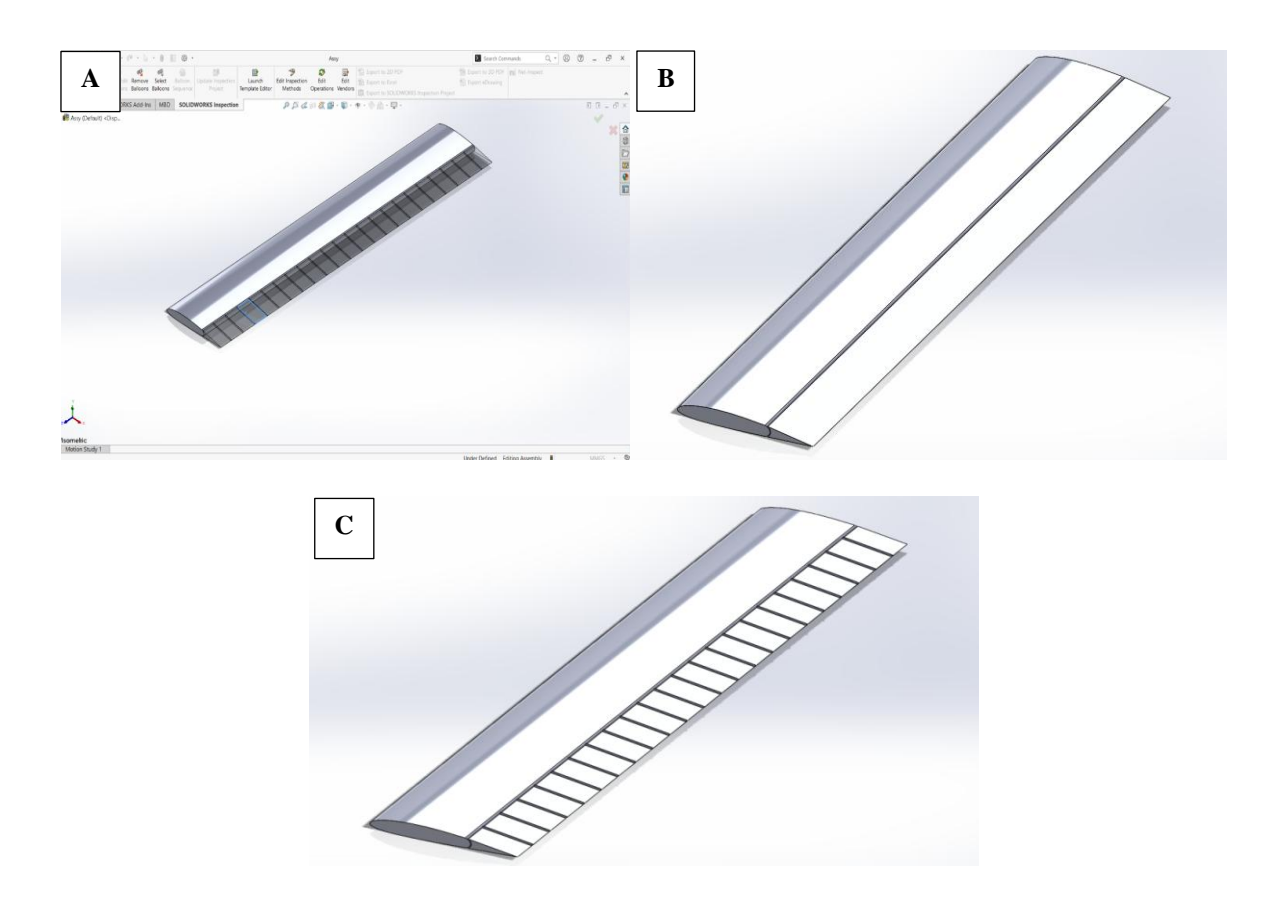


Figure 6. (a) Flaps dan Riblets Merger (b) Wing and Flap (c) Wing, Flap, and Riblets

2.2.1 Research Object Design

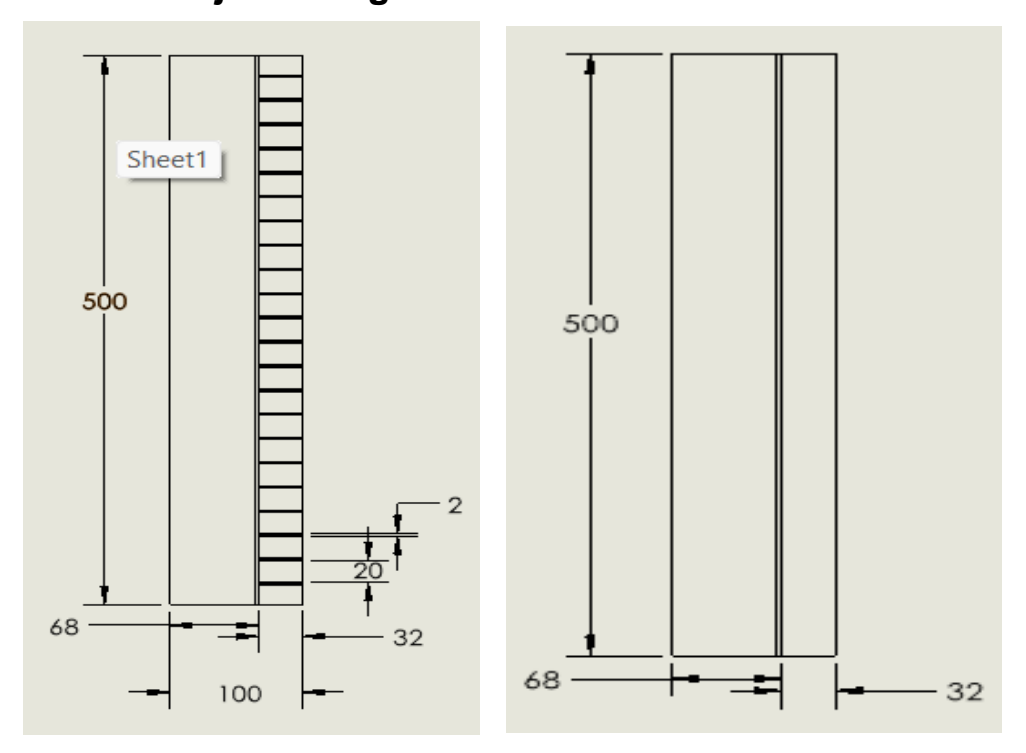


Figure 7. Flap with riblets and flap without riblets

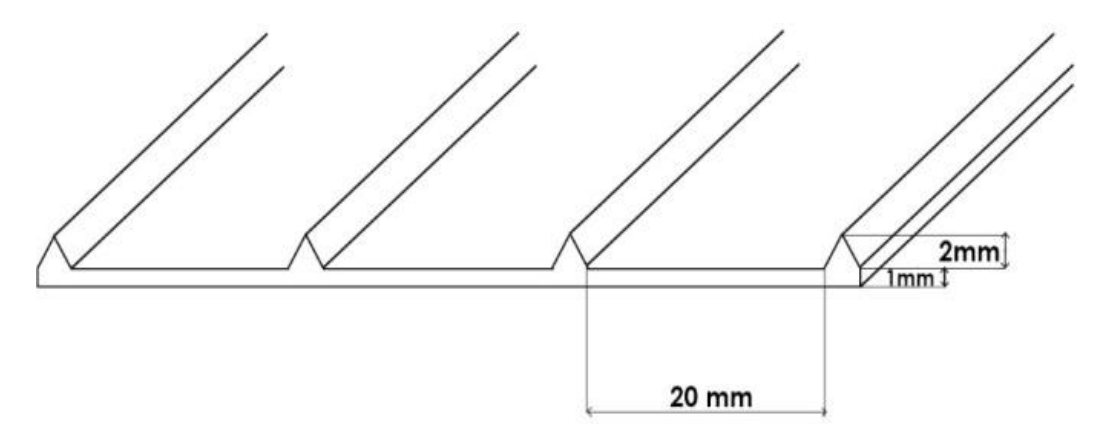


Figure 8. Geometric Modeling of V-Groove Riblets.

2.2.2 Setting boundary conditions on the airfoil geometry

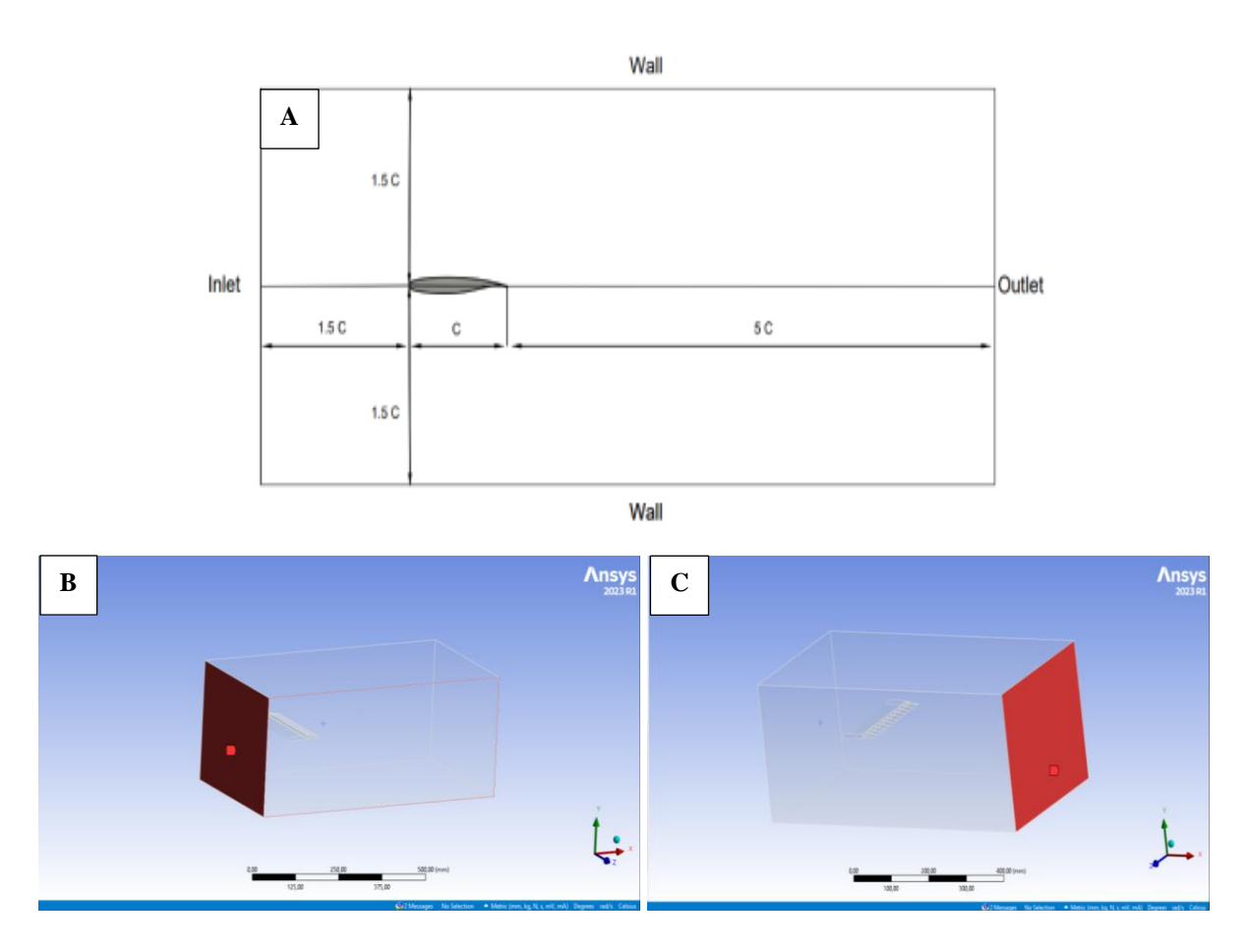
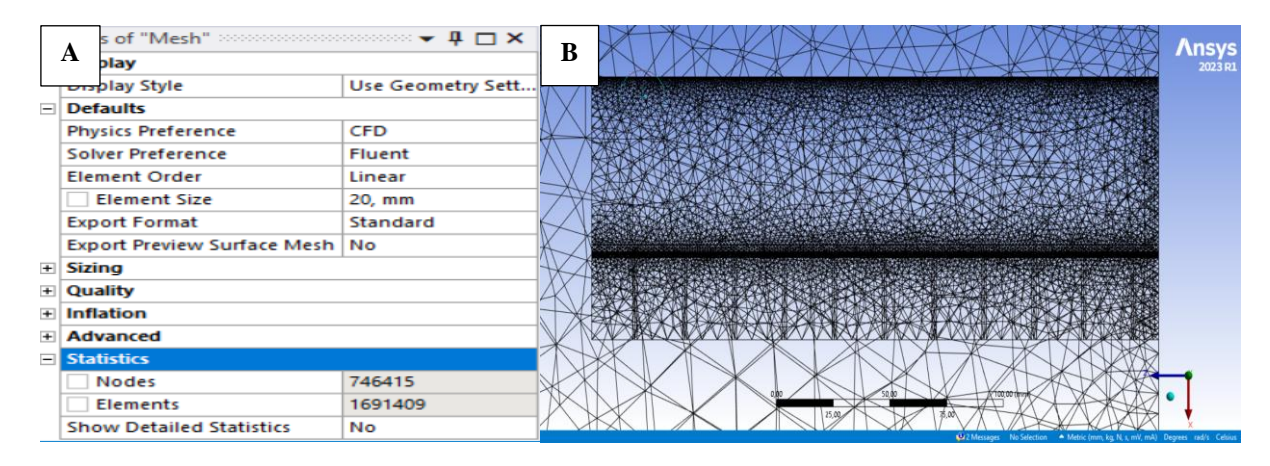


Figure 9. (a) Modeling dimensions and Boundary conditions (b) Inlet Cross Section Inlet velocity to define the incoming flow velocity. (c) Outlet Section Cross Section2.2.1 Meshing

Meshing or discretization in CFD is the process of converting a continuous fluid domain into a discrete computational domain so that the fluid equations can be solved using numerical methods, in this case the Computational Fluid Dynamic (CFD) method. The size functions used are proximity and curvature with fast transitions to reconstruct the details of the riblets.



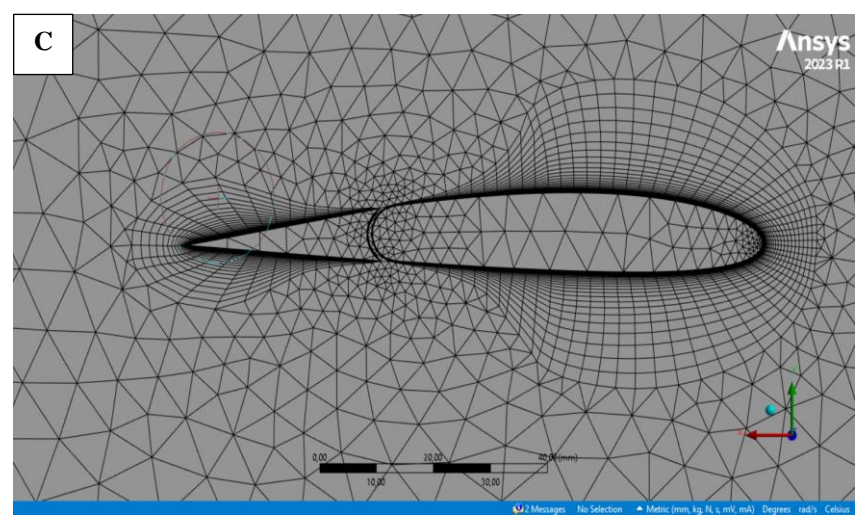


Figure 10. (a) Detail of Mesh (b) Global Meshing Results (c) Meshing Results Around the Wing

2.6 Processing Phase

The processing or solving phase is the stage at which numerical iterations are performed based on the input parameters defined during the pre-processing stage. At this point, the CFD solver executes the calculations iteratively until the specified convergence criteria are satisfied. If convergence is achieved, the process proceeds to the post-processing stage; otherwise, adjustments such as mesh refinement or boundary condition corrections are required before reinitiating the computation. This stage is crucial, as it ensures that the governing equations are solved accurately to capture the flow behavior.

2.7 Post-Processing Phase

The post-processing phase represents the final stage of the simulation, where the results of the numerical analysis are extracted and evaluated. In this study, the simulation outputs were analyzed both quantitatively and qualitatively. The quantitative results included velocity contours and velocity pathlines, while the qualitative analysis involved flow visualization through grid representations, pathlines, contour plots, vector plots, and velocity profiles. These post-processing outputs provide critical insights into the aerodynamic performance and flow characteristics around the modeled airfoil geometry.

3. Results And Discussion

16°

17°

18°

19°

20°

0,98711541

0.94994122

0,90723587

0,89315629

0.86247661

0,99988224

0.98400636

0,95173535

0,94150847

0,90171684

The results of the simulation in this study are in the form of velocity contour and pressure contour on the airfoil so that the *C*I and *C*d values of the NACA 2412 airfoil with riblets and plain can be calculated. The following are the results of simulations that have been carried out at each angle of attack variant:

Angle of	Lift Coefficient			Drag Coefficient		
Attack	Plain	Riblets	Δ	Plain	Riblets	Δ
0°	0,1030316	0,1040597	0,5%	0,140651	0,138564	-0,7%
1°	0,16760264	0,16986888	0,7%	0,144663	0,145146	0,2%
2°	0,23389742	0,23724822	0,7%	0,149397	0,129019	-7,3%
3°	0,29849764	0,30226941	0,6%	0,156066	0,135338	-7,1%
4°	0,36513668	0,36916788	0,5%	0,164060	0,143133	-6,8%
5°	0,43159534	0,4482864	1,9%	0,172764	0,153076	-6,0%
6°	0,4832741	0,48942523	0,6%	0,182231	0,161075	-6,2%
7 °	0,5386313	0,54208442	0,3%	0,192378	0,172337	-5,5%
8°	0,59774822	0,60617977	0,7%	0,203696	0,183307	-5,3%
9°	0,64568025	0,65187628	0,5%	0,215618	0,193924	-5,3%
10°	0,694161	0,71219363	1,3%	0,227865	0,206477	-4,9%
11°	0,75298062	0,7723127	1,3%	0,242413	0,222734	-4,2%
12°	0,79694772	0,80305317	0,4%	0,255881	0,234818	-4,3%
13°	0,84918492	0,87868886	1,7%	0,271468	0,252162	-3,7%
14°	0,90319106	0,95894676	3,0%	0,288115	0,272753	-2,7%
15°	0,94014837	0,96328559	1,2%	0,304377	0,284996	-3,3%

 Table 4. Comparison of Lift Coefficient and Drag Coefficient

It can be seen in tables 6 which show that the greater the angle of attack, the greater the coefficent lift and the greater the drag produced. By adding riblets to the wing airfoil, it succeeds in reducing the coefficent drag and increasing the coefficent lift so that it can improve the performance of the NACA 2412 Airfoil. The maximum lift occurs at α = 14 $^{\circ}$ with an increase of 3% lift coefficent and can reduce drag by 7.3% at α = 2 $^{\circ}$.

0,6%

1,8%

2,4%

2,6%

2,2%

0,322520

0.342662

0,370450

0,378531

0,416711

-3,4%

-3.1%

-3,3%

-2,6%

-2,6%

0,301548

0,321940

0,347053

0,359204

0,395203

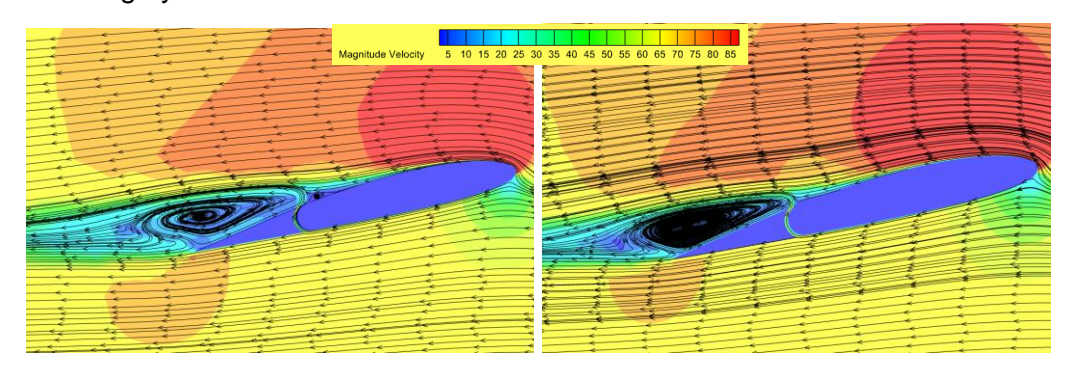


Figure 11. Velocity Contour Flap Visualization using riblets and without using riblets 28

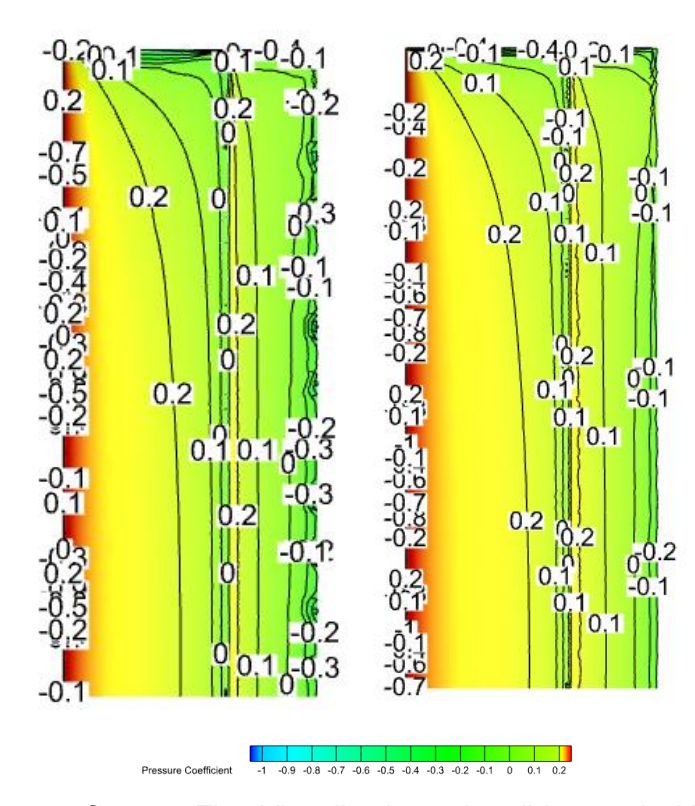


Figure 12. Pressure Contour Flap Visualization using riblets and without using riblets

The simulation results demonstrate that the application of riblets on the flap surface significantly influences the aerodynamic flow characteristics. As illustrated in Figure 11, the presence of riblets reduces the size of vortices formed behind the flap, thereby delaying flow separation compared to the configuration without riblets. This improvement in flow attachment contributes to better aerodynamic performance. Furthermore, the pressure contour analysis in Figure 12 indicates that the flap with riblets experiences lower surface pressure, as shown by the dominance of green shades, whereas the flap without riblets exhibits higher pressure levels represented by yellow shades. The reduction in pressure on the riblet-equipped flap suggests a potential decrease in drag force, aligning with previous studies that riblets enhance boundary layer stability and minimize energy losses. Overall, these findings confirm that integrating riblets into the airfoil flap design can improve aerodynamic efficiency by delaying separation and reducing pressure drag.

Table 6. Coefficient Drag

Angle of	Coefficient Drag Total Plain Wing Airfoil NACA 2412			Coefficient Drag Total Riblets Wing Airfoil NACA 2412			
Attack	Coefficient Pressure	Induce Drag	Friction Drag	Coefficient Pressure	Induce Drag	Friction Drag	
0°	0,012518763	0,000750894	0,12738112	0,012034033	0,000765954	0,12576420	
1°	0,015140193	0,001987007	0,12753601	0,01517493	0,002041105	0,12792975	
2°	0,018054199	0,003869800	0,12747288	0,017390935	0,003981471	0,10764649	
3°	0,022454057	0,006302595	0,12730908	0,021160058	0,006462879	0,10771499	
4°	0,027122895	0,009430800	0,12750615	0,025724417	0,009640186	0,10776864	
5°	0,032030326	0,013176228	0,12755703	0,031094275	0,014215061	0,10776627	
6°	0,037939087	0,016520556	0,12777101	0,036494527	0,016943781	0,10763639	
7°	0,044137818	0,020522052	0,12771844	0,043867435	0,020786026	0,10768399	

8°	0,050641888	0,025274013	0,1277804	0,049675919	0,025992047	0,10763854
9°	0,057979368	0,029489854	0,12814909	0,056254066	0,030058546	0,10761159
10°	0,065658001	0,034084587	0,12812253	0,06318075	0,035878459	0,10741756
11°	0,074060883	0,040105618	0,12824699	0,073167036	0,042191403	0,10737541
12°	0,08279168	0,044925951	0,12816354	0,081887686	0,045616947	0,10731315
13°	0,091854694	0,051008454	0,12860523	0,090336956	0,054614487	0,10721078
14°	0,10195925	0,057702798	0,1284531	0,10062582	0,065046900	0,10708013
15°	0,11331953	0,062521647	0,12853545	0,11250477	0,065636852	0,10685479
16°	0,12508578	0,068924477	0,12850944	0,12404722	0,070718872	0,10678238
17°	0,15004637	0,063830916	0,12878515	0,14706298	0,068490987	0,10638651
18°	0,18376455	0,058220783	0,12846455	0,17644609	0,064072256	0,10653461
19°	0,19372033	0,056427724	0,12838295	0,19016814	0,062702676	0,10633344
20°	0,23516264	0,052617749	0,12893016	0,23134826	0,057514583	0,10633987

The effect of adding v-groove riblets to the flap can produce greater lift than the plain wing. The effect of adding v-groove riblets has a lower drag than plain wing. It can be seen in table 6. shows the highest increase in lift coefficient occurs at $\alpha = 14^{\circ}$ with an increase of 3% lift coefficient and can reduce drag by 7.3% at $\alpha = 2^{\circ}$ so it can be concluded by adding riblets to the airfoil can improve the performance of Airfoil NACA 2412.

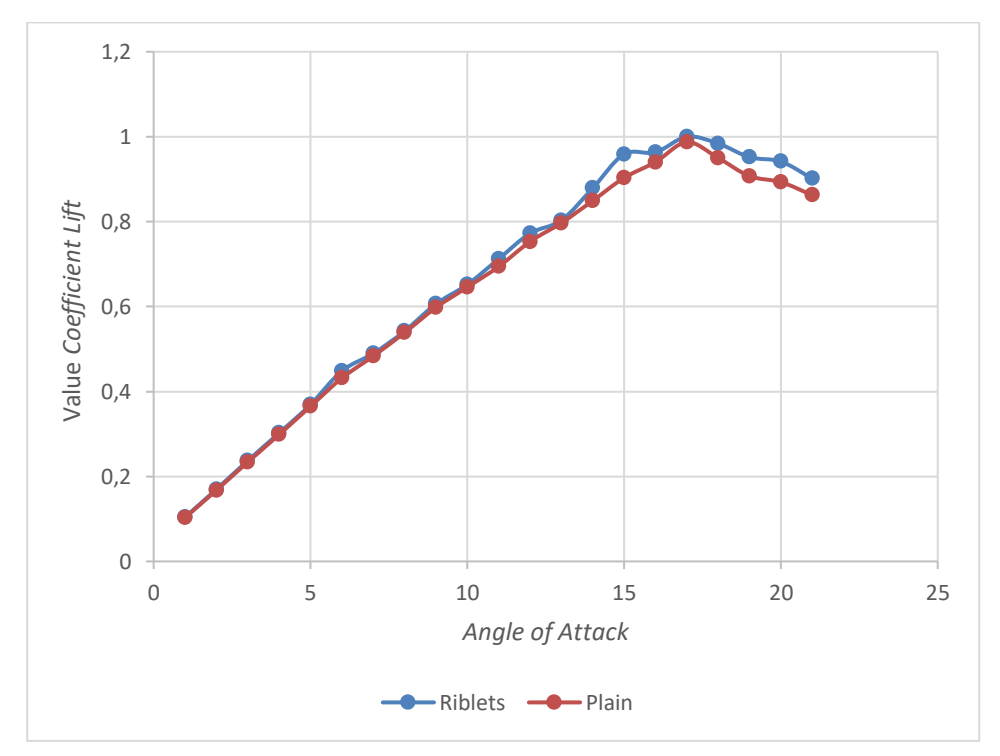


Figure 13. Comparison of Lift Coefficient of Riblets and Plain Wing

Figure 13 shows the lift coefficient of riblets and plain wing airfoil NACA 2412 against the angle of attack. The configuration of adding riblets shows a higher Lift Coefficient value compared to the plain configuration.

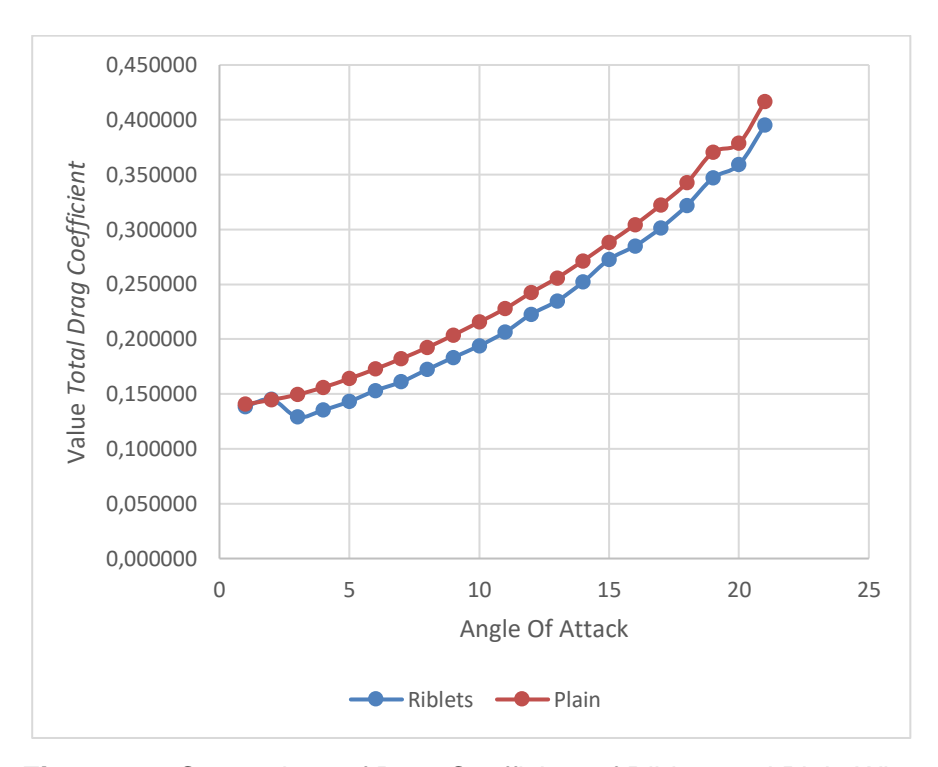


Figure 14. Comparison of Drag Coefficient of Riblets and Plain Wing

Figure 14 shows the Total Drag Coefficient of Riblets and Plain wing airfoil NACA 2412 against angle of attack. Plain wing configuration shows a higher Total Drag Coefficient value compared to the riblets configuration. It can be seen that the position of the plain wing configuration against the flow direction has the largest area compared to the configuration of adding riblets.

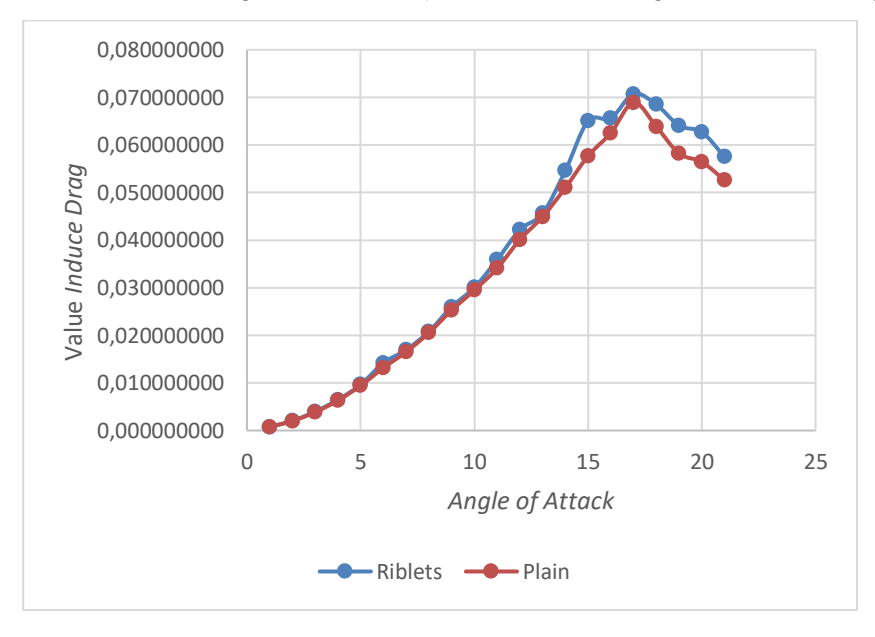


Figure 15. Comparison of Induce Drag of Riblets and Plain Wing

Figure 15 shows the Induced Drag Coefficient of the plain configuration and riblets. Induced Drag Coefficient shows the largest value compared to other types of drag coefficient. Therefore the Total Drag Coefficient and Induced Drag values are very similar because the contribution of Induced

Drag has the largest value to the Total Drag Coefficient compared to other types of drag. The configuration of adding riblets shows a higher value compared to the plain wing configuration.

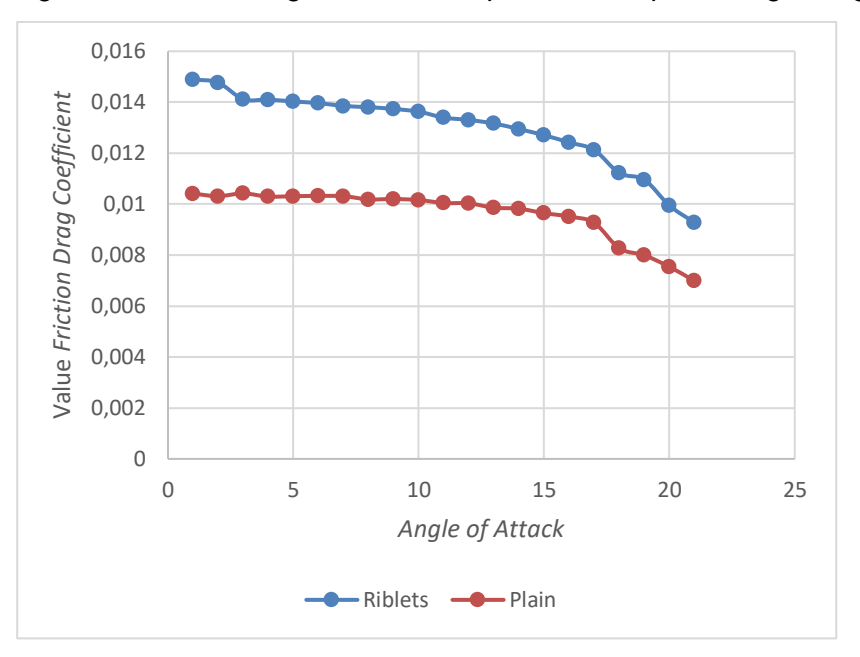


Figure 16. Comparison of Friction Drag of Riblets and Plain Wing

Figure 16 shows the Friction Drag Coefficient of the plain configuration and riblets. The configuration of adding riblets shows a higher value than the plain wing configuration.

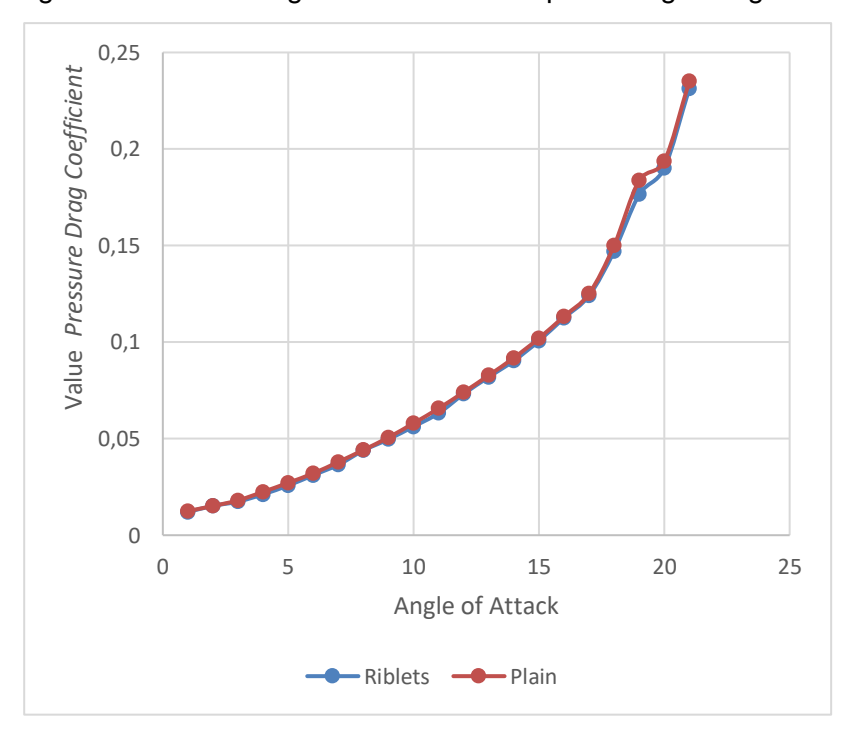


Figure 17. Comparison of Pressure Drag Coefficient of Riblets and Plain Wing

Figure 17 shows the Pressure Drag Coefficient of the plain and riblets configuration. Pressure Drag Coefficient refers to the object area against the airflow direction. The plain wing configuration shows a higher value than the plain wing configuration.

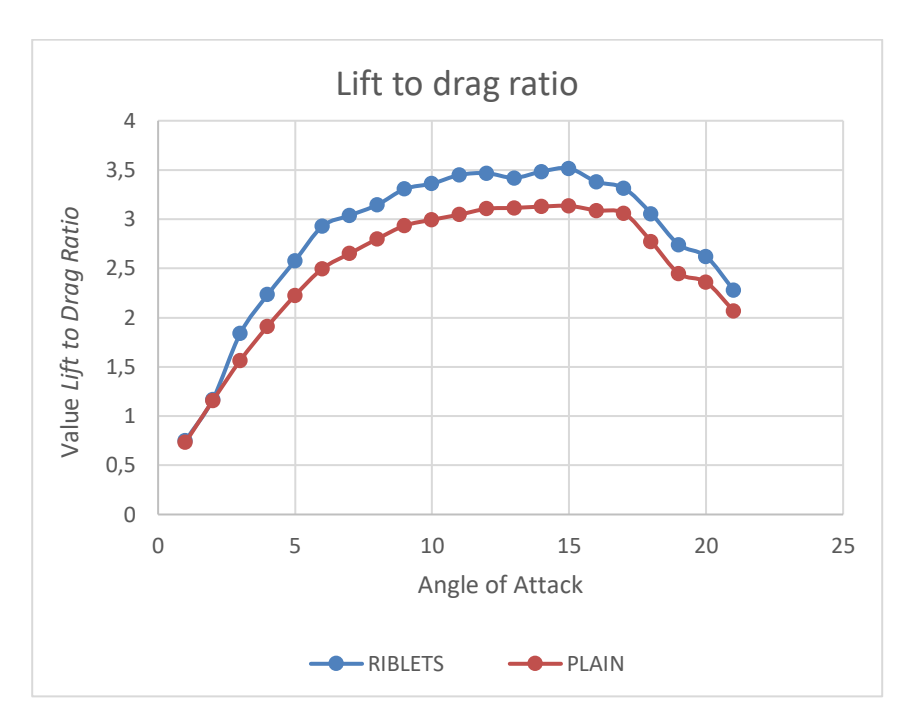


Figure 18. Comparison of Lift to Drag Ratio of Riblets and Plain Wing

Figure 18 shows the results of the Lift to Drag Ratio of the plain configuration and riblets. The configuration of adding riblets produces better performance than the plain wing configuration.

4. Conclusion

Based on the results of the simulations conducted, several key conclusions can be drawn: The addition of v-groove riblets to the NACA 2412 airfoil significantly enhances its performance, with the highest increase in the lift coefficient observed at an angle of attack (α) of 14°, yielding a 3% improvement in lift and a 7.3% reduction in drag at α = 2°. These improvements in aerodynamic performance highlight the beneficial impact of riblet integration on the airfoil's efficiency. Furthermore, the use of v-groove riblets on the flap effectively reduces vortex formation and delays the flow separation point, further contributing to the improved aerodynamic characteristics of the airfoil.

Acknowledgements

The authors gratefully acknowledge the Aircraft Maintenance Department of Politeknik Penerbangan Surabaya for providing the facilities and support for this research. Special thanks are extended to all those who contributed to the experimental process and data analysis.

References

- [1] Dole, C.E.; Lewis, J.E.; Badick, J.R.; and Johnson, B.A. (2017). Flight theory and aerodynamics: A practical guidefor operational safety. John Wiley &Sons, Inc.
- [2] Khan, M.M.I.; and Al-Faruk, A. (2018). Comparative analysis of aerodynamic characteristics of rectangular and curved leading edge wing planforms. American Journal of Engineering Research, 7(5), 281-291.
- [3] Hariyadi, S.P.S.; Junipitoyo, B.; Sutardi; and Widodo, W.A. (2022). Stall behavior curved

- planform wing analysis with low Reynolds number on aerodynamic performances of wing airfoil Eppler 562. Journal of Mechanical Engineering, 19(1), 201-220.
- [4] Torrigiani, F.; Nagel, B.; and Cavallaro, R. (2022). Development of an aeroelastic stability module for wing planform optimization. Proceedings of the 19th International Forum on Aeroelasticity and Structural Dynamics, IFASD 2022, Madrid, Spain.
- [5] Schütte, A.; and Hummel, D. (2022). Impact of planform and control surfaces on the vortical flow topology and roll stability of a multi delta wing configuration. Proceedings of the AIAA AVIATION 2022 Forum, Chicago, IL & Virtual.
- [6] Fouda, M.; and Taha, H.E. (2022). Effect of wing planform on airplane stability and controauthority in stall. Proceedings of the AIAA SCITECH 2022 Forum, San Diego, CA & Virtual.
- [7] Jesudasan, R.; Hanifi, A.; and Mariani, R. (2023). Investigating planar and nonplanar wing planform optimisation for ground effect aircraft. Aerospace, 10(11), 969.
- [8] P. Singh, L. Neuhaus, O. Huxdorf, J. Riemenschneider, J. Wild, J. Peinke, and M. Hölling, "Experimental investigation of an active slat for airfoil load alleviation," Journal of Renewable and Sustainable Energy, vol. 13, no. 4, p. 043304, 2021.
- [9] S. Antoniou, S. Kapsalis, P. Panagiotou, and K. Yakinthos, "Parametric investigation of leading-edge slats on a blended-wing- body UAV using the Taguchi method," Aerospace, vol. 10, no. 8, p. 720, 2023.
- [10] L.W. Traub and M.P. Kaula, "Effect of leading-edge slats at low Reynolds numbers," Aerospace, vol. 3, no. 4, p. 39, 2016.
- [11] S.P. Setyo Hariyadi, B. Junipitoyo, N. Pambudiyatno, Sutardi, and W.A. Widodo, "Aerodynamic characteristics of fluid flow on multiple-element wing airfoil Naca 43018 with leading-edge slat and plain flap," Journal of Engineering Science and Technology, vol. 18, no. 1, pp. 36–50, 2023.
- [12] H. Lv, X. Zhang, and J. Kuang, "Numerical simulation of aerodynamic characteristics of multielement wing with variable flap," Journal of Physics: Conference Series, vol. 916, no. 1, p. 012005, 2017.
- [13] S.P.S. Hariyadi, N. Pambudiyatno, Sutardi, and P.F. Dyan, "Aerodynamic characteristics of the wing airfoil NACA 43018 in take off conditions with slat clearance and flap deflection," in Recent Advances in Mechanical Engineering: Select Proceedings of ICOME 2021. Singapore: Springer Nature Singapore, pp. 220–229, 2022.
- [14] S.H.S. Putro, S. Sutardi, W.A. Widodo, N. Pambudiyatno, and I. Sonhaji, "Effect of leading-edge gap size on multiple-element wing NACA 43018," International Review of Aerospace Engineering, vol. 15, no. 12, pp. 30–40, 2022.
- [15] N.J. Mulvany, L. Chen, J.Y. Tu, and B. Anderson, "Steady-state evaluation of two-equation RANS (Reynolds-Averaged Navier-Stokes) turbulence models for high-Reynolds number hydrodynamic flow simulations," Department of Defence, Australian Government, DSTO Platform Sciences Laboratory, Australia, 2004.
- [16] S. Tobing, "Lift generation of an elliptical airfoil at a Reynolds number of 1000," International Journal of Automotive and Mechanical Engineering, vol. 16, no. 2, pp. 6738–6752, 2019.
- [17] S. Jamei, A. Maimun, N. Azwadi, M.M. Tofa, S. Mansor, and A. Priyanto, "Ground viscous effect on 3D flow structure of a compound wing-in-ground effect," International Journal of Automotive and Mechanical Engineering, vol. 9, pp. 1550–1563, 2014.